

Numerical modeling of moist convection in Jupiter's atmosphere

K. Sugiyama¹, M. Odaka², K. Nakajima³, Y. Morikawa⁴, M. Ishiwatari², K. Kuramoto², and Y.-Y. Hayashi⁵

¹ Institute of Low Temperature Sciences, Hokkaido University, Japan, ² Dept. of CosmoSciences, Hokkaido University, Japan, ³ Dept. of Earth and Planetary Sciences, Kyushu University, Japan,

⁴ National Institute of Information and Communications Technology, Japan, ⁵ Dept. of Earth and Planetary Sciences, Kobe University, Japan

†Contact e-mail: sugiyama@gfd-dennou.org

Introduction

Moist convection is supposed to play important roles in shaping the large scale circulation and distributions of condensable species. However, the convective motion and distribution of condensable species in Jupiter's atmosphere has not been clarified yet.

Previous numerical studies

- Atreya and Romani (1985) estimated the vertical profiles of cloud density by using a one-dimensional thermodynamic equilibrium cloud condensation model (Fig. 1).
- Yair *et al.* (1992, 1995) and Hueso and Sanchez-Lavega (2001) performed a numerical simulation of an isolated cloud thermal.
- Nakajima *et al.* (2000) and Sugiyama *et al.* (2009) examined vertical atmospheric structure established through a large number of life cycles of convective cloud and showed that the thin stable layer associated with H₂O condensation acts as a boundary for vertical convective motion (Fig. 2, 3).

In this study

- The results given by Nakajima *et al.* (2000) and Sugiyama *et al.* (2009) may quite possibly be due to the unrealistically large strength of the given radiative forcing that is set to be about 100 times larger than that estimated for the actual atmosphere of Jupiter.
- For the purpose of understanding the variety of structures of cloud convection that can be established in Jupiter's atmosphere, we perform a long-term numerical simulation with fixed thermal forcing, and examine distribution of condensable species and convective motion.
- The dependency of these structure on the radiative forcing and the abundances of condensable volatiles are also shown.

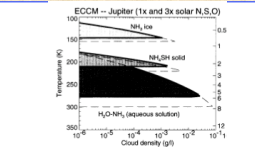


Fig. 1 Vertical structure of Jupiter's cloud obtained by the equilibrium cloud condensation model (Atreya *et al.*, 1999).

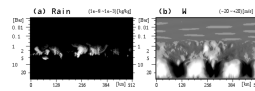


Fig. 2: The results of numerical simulation by Nakajima *et al.* (2000). Distribution of H₂O rain water mixing ratio (left) and vertical velocity (right). The convective motion is separate at the water condensation level.

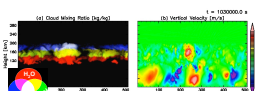


Fig. 3: The results of numerical simulation by Sugiyama *et al.* (2009). Distribution of rain water mixing ratio (left) and vertical velocity (right). The convective motion is separate at the water condensation level. The mixing ratios of H₂O, ice, NH₄SH, and NH₃ are represented using red, green, and blue color tones, respectively, and that of multiple composition cloud is represented by a superposed plot of the three colors.

Numerical Model

The basic equations of the model are based on the quasi-compressible system (Klemp and Wilhelmson, 1978) and conservation equations of condensible species.

- The cloud microphysics are implemented by the parameterization schemes of Kessler (1969).
- The conversion rate due to accretion and fall velocity of rain is specified as three times the value used in terrestrial case considering strong gravity and small air density in Jupiter's condition (Cf. Yair *et al.*, 1995).
- The effect of subgrid turbulence are implemented by the parameterization schemes of Klemp and Wilhelmson (1978).

Set-up of Experiments

Model settings are shown by Fig. 4 and Table 1.

- The computational domain extends to 1024 km horizontally and 300 km vertically. The grid interval is 2.0 km.
- The atmosphere is cooled (Q_{rad}) between 140 km (2 bar) and 200 km (0.1 bar) at a constant rate of -0.01 or -0.1 K/day.
- Boundary conditions
 - Horizontal boundary is cyclic. Stress free condition and $w = 0$ are given at the lower and upper boundaries.
 - Temperature and mixing ratios of vapor at the lowest level are fixed.
- Initial condition
 - The isentropic atmosphere ($T=160K$ at $p=0.6bar$) is assumed from 30 to 0.1 bar, and isothermal above 0.1 bar (100 K).
 - Deep abundances of vapor (H₂O, NH₃, and H₂S) are set to be 0.3, 1, 3, and $10 \times$ solar taken from Asplund *et al.* (2005). Mixing ratios are reduced in the "cloud" layers so that the relative humidities do not exceed 75%.
 - Random potential temperature perturbation ($\Delta\theta_{max} = 0.1$ K) is given to seed convective motion.

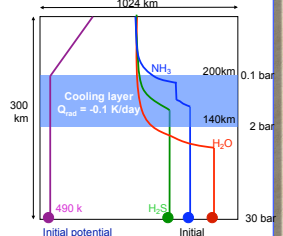


Fig. 4: Schematic figure of model settings.

Table 1: The list of parameters

Name	Control	R10	R10S1	R10S3	R10S10
Grad (K/day)	-0.01	-0.1	-1	-0.1	-0.1
abundance (solar)	1.0	1.0	1.0	0.1	3.0
					10.0

Results

Control:

- Time evolution of the horizontal and vertical mean latent heating rate showing distinct temporal intermittency indicates that active cloud convection occur periodically (Fig 5).
- The atmospheric structure may be considered to reach a state of statistical equilibrium over the time scale of the periodic intermittency.
 - The values of the vertical cloud distribution and virtual potential temperature also changes periodically (Fig 5).
- In the period of active cloud development, the H₂O and NH₄SH cloud and rain particles can be advected to the tropopause (Fig 6).
 - H₂O condensation level acts as a kinematic and compositional boundary.
- In the quiet period, the altitudes of the lowest cloud bases are different from those in the period of active cloud development (Fig 6).
 - Horizontally spread NH₃ cloud layer is shown.
 - NH₃ clouds and the mixed cloud that consists of H₂O and NH₄SH cloud particles are also shown.
 - NH₃ condensation level acts as a kinematic and compositional boundary.

The dependency of the strength of radiative forcing:

- The distinct temporal intermittency is shown in R10 (Fig 7).
 - The durations of the active period in R10 and Control are almost the same, 2-3 days.
- The characteristic of vertical atmospheric structure and convective motion in R10 is almost the same as that in Control.
- The difference between Control and R10 is that the characteristic shown by Fig 6 (a-2) is not seen in the quiet period of R10.
- The characteristic of vertical atmospheric structure and convective motion in R100 is the same as that in the active period of Control.

The dependency of the amount of condensable component in the sub-cloud layer:

- In this comparison, R10 is treated as the standard case in order to reduce CPU time required to achieve a statistical equilibrium state in the model atmosphere.
- The distinct temporal intermittency is shown in R10S3 and R10S10 (Fig 7).
- The NH₃ condensation level and the NH₄SH reaction level act as such dynamical boundaries in the quiet period of R10S10 (Fig 8).
- The stable layer associated with H₂O condensation is weak in R10S01, so that the H₂O condensation level acts as a weak boundary for vertical convective motion (Fig 9).

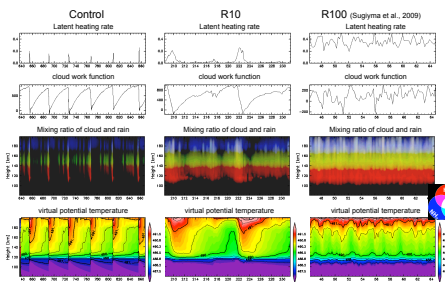


Fig. 5: Time evolution of horizontal and vertical mean latent heating rate (a), cloud work function (b), horizontal mean cloud and rain mixing ratio (c), and horizontal mean virtual potential temperature shown in Control, R10, and R100. Mixing ratios of cloud and rain shown by (c) are represented by logarithmic scale ranging from 10^0 to 10^3 kg/kg. Images in H₂O ice (red), in NH₄SH (green), in NH₃ ice (blue) are superposed.

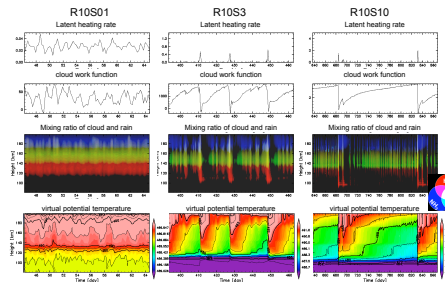


Fig. 7: The same figure of Fig. 5 but for R10S01, R10S3, and R10S10.

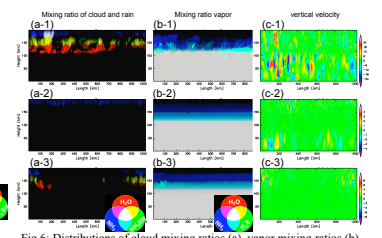


Fig. 6: Distributions of cloud mixing ratios (a), vapor mixing ratios (b), and vertical velocity (c) shown in Control. Frames (a-1), (b-1), and (c-1) show distributions for the active period, and the remaining 6 frames are for the quiet period. Cloud mixing ratios are plotted on a logarithmic scale having range of $1.0e-8$ -- $5e-4$ kg/kg. Vapor mixing ratios are plotted on a linear scale normalized to the initial values. Images in H₂O ice and vapor (red), in NH₄SH and H₂S vapor (green), in NH₃ ice and vapor (blue) are superposed.

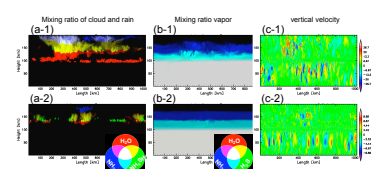


Fig. 8: The same figure of Fig. 6 but for R10S10. Frames (a-1), (b-1), and (c-1) show distributions for the active period, and the remaining 3 frames are for the quiet period.

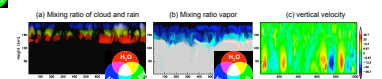


Fig. 9: The same figure of Fig. 6 but for R10S01

Discussion

The period is roughly estimated by using temperature deviation and radiative cooling rate.

- The following expressions is satisfied if the latent heating balances the radiative cooling.

$$\int_{p_{base}}^{p_{top}} \rho c_p \Delta T \Delta z = \int_{p_{base}}^{p_{top}} \rho c_p Q_{rad} \Delta z \Delta t$$

- ρ : density, c_p : specific heat, z : altitude, Q_{rad} : radiative cooling, t : period
- p_{top} : pressure of the tropopause, p_{base} : pressure of the H₂O cloud base, p_{rad} : pressure of the bottom of radiative region
- The following approximated equation can be used when we assume that c_p and ΔT are constant, $p_{top} \ll p_{cloud} \ll p_{rad}$, and hydrostatic equilibrium is satisfied,

$$\Delta t = (\Delta T / Q_{rad}) (p_{cloud} / p_{rad}) \quad (1)$$

The period of the "active/break" cycle is roughly proportional to the amount of condensable component in the sub-cloud layer (Table 2).

- The period of Control is not 10 times larger than that of R10, whereas the radiative cooling rate of Control is 1/10 times larger than that of R10 (Table 2).
 - The virtual potential temperature just before the active period of Control is high than that of R10 (Fig 5)
 - The computational domain of Control is too small?

The condition to start of active cloud convective activity:

- A down flow from the upper troposphere can reaches to the H₂O condensation level.
- The value of the virtual potential temperature is almost the same above H₂O condensation level.

The condition to start of active cloud convective activity:

- A relatively heavy air parcel that consists of many condensable volatiles can not rise from H₂O condensation level to the tropopause.
- The value of cloud work function is almost zero at the end of the active cloud development (Fig 5, 7).
- Cloud work function A is defined as a vertical integration of work by buoyancy per unit mass flux ("the kinetic energy generation per unit mass flux", Arakawa and Schbert (1974)), this can be written in equation form,

$$A = \int \rho g (T_v^* - T_v) / T_v dz \quad T_v: \text{virtual temperature, } * \text{ means air parcel}$$

Table 2: Summary on the period of cloud activity

	period in the numerical experiment (day)	period based on eq. 1 (day)	ratio to the period of R10	abundance of condensable volatiles (solar)	radiative cooling rate (K/day)
Control	36.4	35.4	0.26	1.0	-0.01
R10	9.3	8.8	1	1.0	-0.1
R10S3	19.5	23.5	2.1	3.0	-0.1
R10S10	109.4	110.3	11.8	10.0	-0.1

Concluding Remarks

The most important findings from our calculations are

- Quasi-periodic temporal variation of the convective cloud activity exists in Control, R10, R10S3, and R10S10.
- The period of the quasi-periodic cycle is roughly proportional to the abundance of water vapor in the sub-cloud layer,
- It should also be remarked that the clouds structure given by the numerical simulation is different from the classical three clouds layers structure (Fig. 1) that has been expected by one-dimensional thermodynamic equilibrium

This correspondence between the deep volatile abundance and temporal variability of cloud convection implies a new method to "probe" the deep atmosphere.

Acknowledgements

Long-time numerical simulation of cloud convection are performed by using XT-4 at the National Astronomical Observatory of Japan. We thank softwares developed by many other members of GFD Dennou Club such as Dennou Club Library (DCL), products of Dennou Ruby Project, and gtools library. The numerical model that is used in this study is available from the following URL: <http://www.gfd-dennou.org/library/deepconv/>